Behavior of a Falling Paper

Yoshihiro Tanabe and Kunihiko Kaneko

Department of Pure and Applied Sciences, University of Tokyo, Komaba, Meguro-ku, Tokyo 153, Japan

(Received 29 March 1994)

Behavior of a falling paper in a two-dimensional fluid is investigated by introducing a simple phenomenological model including the lift and friction terms. Five falling patterns are discovered with the increase of friction coefficients: periodic rotation, chaotic rotation, chaotic fluttering, periodic fluttering, and simple perpendicular fall. Irregular motions of the fall are explained in terms of low-dimensional chaos.

PACS numbers: 47.52.+j, 05.45.+b

Anybody must have noticed that the falling motions of a paper or a leaf are very complex. Indeed, in daily life various motions are observed when one drops a light and thin body such as a paper or leaf. Sometimes a falling paper's motion may seem to be *random*. Sometimes it looks very *regular*. It may fall, for example, downward in one direction with rotations, while rarely fluttering to the right and left. It is quite natural to wonder whether these irregular motions are chaotic or not.

Thus far, however, there has been no answer to this question. A possible reason for the absence of the studies to answer this question lies in the difficulty of the problem: One must take into account the complex interactions between the air (fluid) and the paper. The most direct approach is the use of the Navier-Stokes' equation with time dependent boundary conditions. This, however, requires an extremely large amount of computer resources even if some approximations are adopted.

In the present paper we introduce a simple model for a falling paper from a different view. Only the indispensable minimum information from fluid mechanics is taken into account. Although this approach may be a crude approximation, one may be able to construct a model with only a few variables, by which we can answer whether chaos can explain irregular motions of a falling paper. We will show that the dynamics of a falling paper can be reproduced qualitatively well by a simple model. For the modeling we make the following assumptions.

Here, we consider a two-dimensional case, and we will assume that the motions take place in an X-Y plane.

(1) The paper is treated as a rigid body, whose thickness is assumed to be 0. Thus the body is characterized only by its length l and mass m_p.

(2) The paper is subjected to three forces: lift, friction, and gravity. For the calculation of lift, we assume that the fluid is incompressible and perfect. Since the perfect fluid does not bring any friction, we add the phenomenological friction force *ad hoc*. To be specific, the lift and friction terms are calculated as follows.

(2.1) *Lift*: By the assumption (2) we can use the theory of a two-dimensional incompressible perfect fluid. By the celebrated Kutta-Joukowski's theorem, lift can be calculated if a uniform flow of fluid blows at a static object [1]. Assuming that the fluid motion is stationary at each moment, the lift is thus calculated by making the Galilean transformation to the frame at which the velocity of the paper is zero.

(2.2) *Friction*: The Kutta-Joukowski's theorem also tells us about drag, but it is zero. In order to include the friction seen in a real (viscous) fluid, we introduce friction terms proportional to the velocity of the paper [2].

It is natural, in general, to assume that the components of the friction perpendicular and parallel to the paper are *not* equal. The friction will be small if the paper is oriented parallel to the direction of fall, and large if the paper is oriented perpendicularly to the direction of fall. Thus we include two friction coefficients $k_\perp$ and $k_\parallel$ per unit mass. The former gives the friction against the motion perpendicular to the paper, while the latter corresponds to the parallel motion.

Using (1) and (2) we can construct our model as follows. Let (x, y) denote the position of the center of mass, (u, v) the velocity in the X-Y plane ($u = \dot{x} \equiv dx/dt, v = \dot{y} \equiv dy/dt$, t : time), θ the angle of the paper, and $\omega (= \dot{\theta})$ the corresponding angular velocity. See Fig. 1. The motions of a paper are described by these variables.

By the assumption on the friction terms, the components of the friction force perpendicular and parallel to the paper are straightforwardly obtained as:

$$F_\perp = -m_p k_\perp (v \cos\theta - u \sin\theta),$$

$$F_\parallel = -m_p k_\parallel (v \sin\theta + u \cos\theta),$$

where m_p is the mass of the paper. Thus, the friction at the center of mass is given by

$$\begin{aligned} F_x &= -F_\perp \sin\theta + F_\parallel \cos\theta \\ &= m_p[-(k_\perp \sin^2\theta + k_\parallel \cos^2\theta)u \\ &\quad + (k_\perp - k_\parallel)\sin\theta\cos\theta v], \\ F_y &= F_\perp \cos\theta + F_\parallel \sin\theta \\ &= m_p[(k_\perp - k_\parallel)\sin\theta\cos\theta u \\ &\quad - (k_\perp \cos^2\theta + k_\parallel \sin^2\theta)v], \end{aligned} \tag{1}$$

0031-9007/94/73(10)/1372(4)$06.00

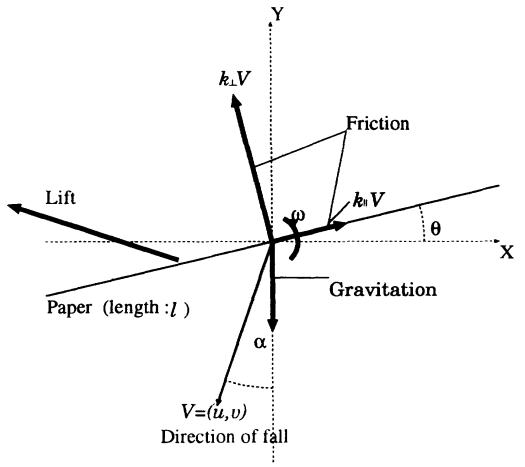

FIG. 1. Schematic illustration of the paper and the forces.

while the friction to the rotation is given by

$$F_\theta = -m_p k_\perp l^2 \omega/12. \tag{2}$$

With the help of the Kutta-Joukowski's theorem, a plate in a flow of the velocity U with the angle ϕ is subjected to the lift $L = l\rho_f \pi U^2 \cos\phi$, and the moment $M = -Ll \sin\phi/4$, where ρ_f is the density of the fluid. Using the Galilean transformation, we obtain the lift and momentum of the paper in Fig. 1 as follows:

$$\begin{aligned} L_x &= \mp l\rho_f \pi V^2 \cos(\alpha + \theta)\cos\alpha, \\ L_y &= \pm l\rho_f \pi V^2 \cos(\alpha + \theta)\sin\alpha, \\ M &= -l^2\rho_f \pi V^2 \cos(\alpha + \theta)\sin(\alpha + \theta)/4, \end{aligned} \tag{3}$$

here, $V \equiv \sqrt{u^2 + v^2}$, $\alpha \equiv \arctan(u/v)$ and the upper [lower] sign denotes the condition ($v < 0$, $0 < \alpha + \theta < \pi$) or ($v > 0$, $-\pi < \alpha + \theta < 0$) [($v < 0$, $-\pi < \alpha + \theta < 0$) or ($v > 0$, $0 < \alpha + \theta < \pi$)]. Combining the lift and friction terms and the gravity force [Eqs. (1), (2), and (3)], we obtain the following set of ordinary differential equations governing the motion of the paper:

$$\begin{aligned} \dot{u} &= -(k_\perp \sin^2\theta + k_\parallel \cos^2\theta)u + (k_\perp - k_\parallel) \\ &\quad \times \sin\theta\cos\theta v \mp \pi\rho V^2 \cos(\alpha + \theta)\cos\alpha, \\ \dot{v} &= (k_\perp - k_\parallel)\sin\theta\cos\theta u - (k_\perp \cos^2\theta + k_\parallel \sin^2\theta)v \\ &\quad \pm \pi\rho V^2 \cos(\alpha + \theta)\sin\alpha - g, \\ \dot{\omega} &= -k_\perp \omega - (3\pi\rho V^2/l)\cos(\alpha + \theta)\sin(\alpha + \theta), \\ \dot{\theta} &= \omega, \end{aligned} \tag{4}$$

where ρ is the ratio of the density of the fluid to that of the paper ($\rho \equiv \rho_f l/m_p$).

We have carried out the numerical integration of Eqs. (4) with the fourth order adaptational Runge-Kutta method.

In our model, we have found five basic falling patterns with the change of parameters $k_\perp$, $f(\equiv k_\perp/k_\parallel)$, ρ, and l.

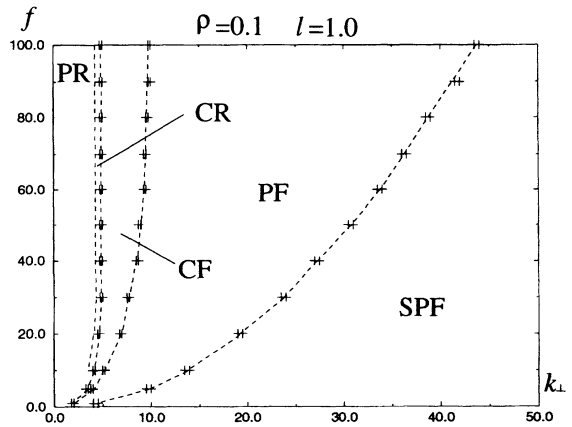

FIG. 2. Phase diagram at $\rho = 0.1$ and $l = 1.0$ m. There are five falling patterns: PR (periodic rotation), CR (chaotic rotation), CF (chaotic fluttering), PF (periodic fluttering), and SPF (simple perpendicular fall). For larger f ($\equiv k_\perp/k_\parallel$) the patterns can clearly be distinguished. As f gets smaller, the chaotic regions become narrower and finally disappear at $f \simeq 1.0$.

A phase diagram against the change of $k_\perp$ and f is shown in Fig. 2.

If $k_\perp$ is small enough, the paper falls regularly to the right side (left side) with a counterclockwise (clockwise) rotation after the transients have died out. The direction of rotation depends on the initial condition. Hereafter we call this *periodic rotation* (PR). The falling pattern of the paper is given in Fig. 3. As $k_\perp$ is increased, a period doubling cascade is observed as the period of the rotation. The orbit of a period-8 limit cycle is plotted in the u-v plane in Fig. 4.

If we increase $k_\perp$ further, the u-v plot gets much denser, while the falling pattern of the center of mass appears similar to the one of PR. We have calculated the maximum Lyapunov exponent to determine whether the system is chaotic or not. The exponent turns out to be positive, hence implying that the motion is chaotic. The

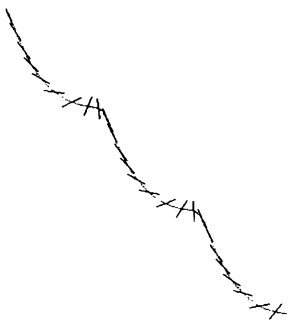

FIG. 3. The locus of the falling paper at the PR regime within the period-1 region. $k_\perp = 4.0$, $f = 100$, $\rho = 0.1$, and $l = 1.0$ m. Each dot denotes the center of mass by a time interval of 0.01 s, while the paper is drawn every 0.1 s.

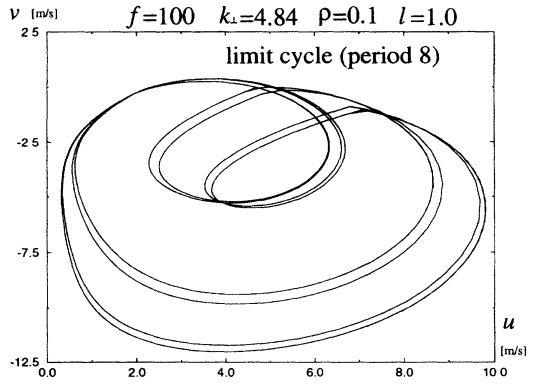

FIG. 4. The u-v plot of the period-8 region with $k_\perp = 4.84$, $f = 100$, $\rho = 0.1$, and $l = 1.0$ m, after transients have decayed.

strange attractor in the $u - v$ plane is plotted in Fig. 5. Hereafter we call this *chaotic rotation* (CR).

The parameter region providing CR is not wide. When $k_\perp$ is increased a little bit more, the paper falls downward swaying right and left chaotically. Hereafter we call this *chaotic fluttering* (CF). See Fig. 6 for the orbit in the u-v plane. Note that the symmetry with respect to the right and left direction is restored here. The horizontal displacement $\delta x(t)$ during the fall of t seconds are well described by the random walk. Indeed the distribution of $\delta x(t)$ is well fit by $P(\delta x) \propto \exp[-(\delta x)^2/4Dt]$ with the diffusion constant D ($D \approx 13.8$ m^2/s for $k_\perp = 6.0$). Note that the displacement is proportional to time t in the PR and CR regimes. When $k_\perp$ is increased further, a transition to regular motions via intermittency is observed. The portion of regular motions becomes larger with the increase of $k_\perp$. An example of the locus of the fall is given in Fig. 7.

For larger $k_\perp$, the motion becomes regular again. The paper sways to the right and left regularly, as is shown in Fig. 8. The orbit depicts a figure eight in the u-v plane. We call this *periodic fluttering* (PF).

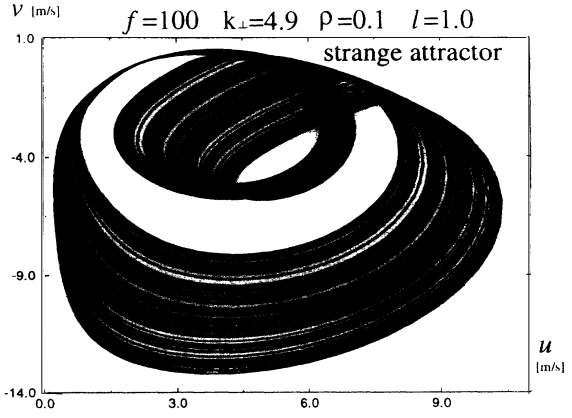

FIG. 5. Strange attractor projected to the u-v plane in CR with $k_\perp = 4.9$, $f = 100$, $\rho = 0.1$, and $l = 1.0$ m.

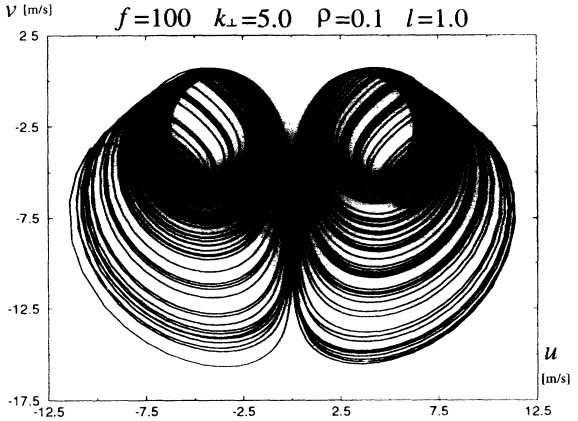

FIG. 6. Strange attractor projected to the u-v plane in CF with $k_\perp = 5.0$, $f = 100$, $\rho = 0.1$, and $l = 1.0$ m.

The amplitude of the sway decreases with the further increases of $k_\perp$, until it finally becomes zero. The paper then falls perpendicularly, without any horizontal motion. In other words, $u = \omega = \theta = 0.0$ and $v = -g/k_\perp$ as time goes to infinity. We call this *simple perpendicular fall* (SPF) [3]. A large value of $k_\perp$ implies a strong viscosity. This fall can be easily understood by imagining the fall of a needle in honey.

The maximum Lyapunov exponent is plotted with the change of $k_\perp$ in Fig. 9. We note that some drops are visible within the CF region, corresponding to windows. At the largest window seen in Fig. 9, the locus is plotted in Fig. 10. The horizontal symmetry is again broken as in PR and CR, although this falling pattern itself is rather similar to PF.

For $\rho = 0.1$ and $l = 1.0$ m, the attractor is unique except for the right/left choices in PR and CR regimes. When ρ or l is decreased, we have seen coexistences of

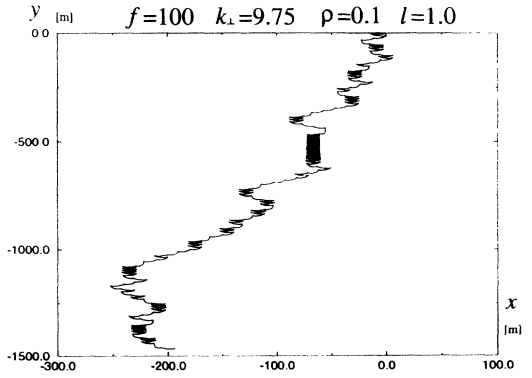

FIG. 7. The motion of the center of mass in CF with $k_\perp = 9.75$, $f = 100$, $\rho = 0.1$, and $l = 1.0$ m, plotted over 600.0 s. The initial condition is set to $u = 0.0$, $v = 0.0$, $\omega = 0.0$, and $\theta = 1.0$.

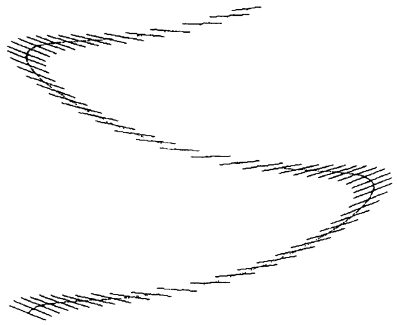

FIG. 8. The locus of the falling paper in PF with $k_\perp = 10.0$, $f = 100$, $\rho = 0.1$, and $l = 1.0$ m. Each dot denotes the center of mass with a time interval of 0.01 s, while the paper is drawn every 0.1 s.

different types of fall for some regions. For example, PF, CF, and CR coexist depending on the initial condition for $k_\perp \simeq 5.5, f = 100, \rho = 0.01$, and $l = 1.0$ m.

To sum up, we have succeeded in constructing a simple model reproducing a variety of falling patterns observed in daily life. Through this model, we are able to demonstrate that irregular motions of a falling paper are explained in terms of low-dimensional chaos. Five falling patterns (periodic/chaotic rotation/fluttering and simple perpendicular fall) are successively found with the change of just the friction coefficients. We also note that this variety of falling patterns is possible only if $k_\perp$ is larger than $k_\parallel$.

Since our model, despite its simplicity, includes essential interactions in the falling motions in fluid, similar behaviors as ours are expected to be found in real experiments with more complex situations (including a fall of two-dimensional sheet in a three-dimensional fluid). In particular, one can make a quasi-two-dimensional experiment: Prepare a thin flat object in fluid sandwiched by two parallel plates, then drop it. With a controlled experiment, it will be possible to confirm the bifurcation and chaos in the fluttering fall, by changing the length or the density of the object, or a physical property of the fluid such as its density or viscosity.

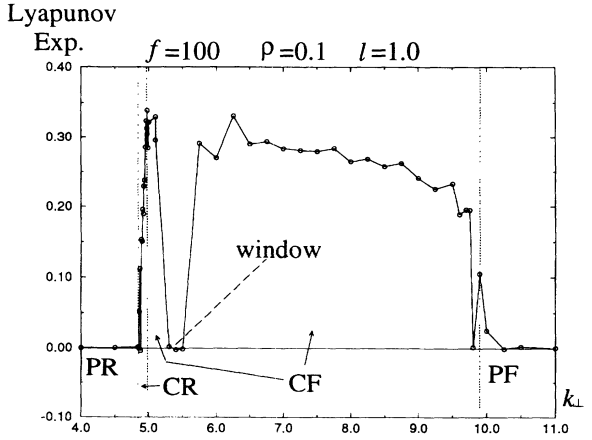

FIG. 9. Plots of the maximum Lyapunov exponent versus $k_\perp$. The parameters are set to $f = 100$, $\rho = 0.1$, and $l = 1.0$ m.

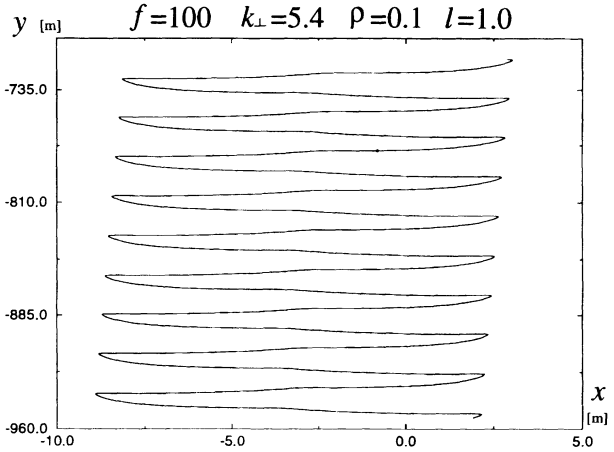

FIG. 10. The x-y plot for a time interval of 60 s. The paper falls regularly as if the paper were subjected to wind.

The authors would like to thank F.H. Willeboordse for a critical reading of the manuscript and the illuminating discussions and K. Tokita and T. Yamamoto for useful discussions. The present work is partially supported by a Grant-in-Aid for Scientific Research on Priority Areas from the Ministry of Education, Science and Culture, Japan.

[1] L. M. Milne-Thomson, *Theoretical Hydrodynamics* (Macmillan, London, 1972), pp. 200 and 201.

[2] L. M. Milne-Thomson, *Theoretical Hydrodynamics* (Ref. [1]), pp. 681 and 682: When the velocity of an object in fluid (i.e., the Reynolds number) is small, Stokes' approximation is valid, and the friction is proportional to the velocity.

[3] The bifurcation from SPF to PF is associated with the appearance of the imaginary eigenvalue of the Jacobi matrix around the fixed point solution, but differs from the Hopf bifurcation due to the discontinuity by the two signs in Eqs. (3).

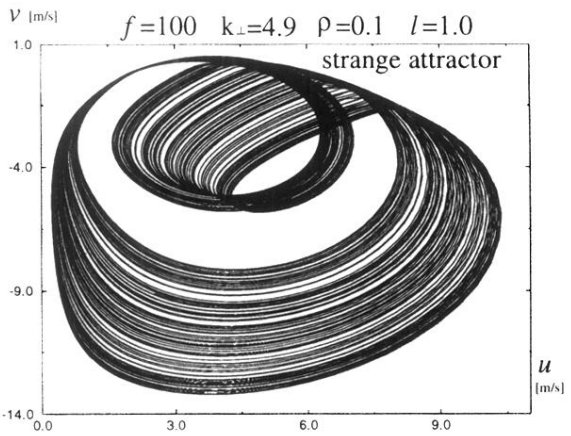

FIG. 5. Strange attractor projected to the u-v plane in CR with $k_\perp = 4.9$, $f = 100$, $\rho = 0.1$, and $l = 1.0$ m.

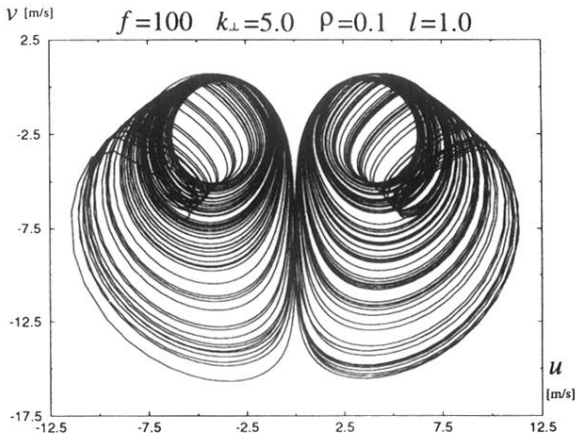

FIG. 6. Strange attractor projected to the u-v plane in CF with $k_\perp = 5.0$, $f = 100$, $\rho = 0.1$, and $l = 1.0$ m.